Drying shrinkage of alkali-activated concrete -State-of-the-art

a research study into the mechanisms, the influencing factors, and mitigation strategies of drying shrinkage of alkali-activated concrete.

By

A. Abbasi

In Partial Fulfilment of the Requirements for the Degree of

BSc. in Civil Engineering

at The Delft University of Technology

October 2020

Supervisor: Dr. G. Ye, TU Delft 2nd supervisor: Dr. H. Dong, TU Delft



Preface

This thesis was written to fulfill the graduation requirements of the Bachelor of Civil Engineering program at the Delft University of Technology. It was completed within two months of work (researching and writing), from September to October 2020.

This research is proposed to provide guidelines for the development of crack-resistant AAC in structural/non-structural applications. Reading this report will give the reader the knowledge they need to begin researching in drying shrinkage in alkali-activated concrete.

Besides the fact that the topic is too big to be covered in just two months of work, the topic was entirely new for me. However, my supervisors' high interest in this topic and their support motivated me and made me more interested in this topic. Therefore, I would like to thank them (Dr. Guang Ye and Dr. Hua Dong) very much for their excellent guidance and support during this research.

The Hague, October 2020

Anas Abbasi

Abstract

Alkali-activated concrete (AAC) has emerged as an environmentally friendly alternative to conventional concrete, as It is a cement-free concrete made by activating precursors (mainly low-cost, low-CO₂ industrial by-products) with alkalis. AAC has demonstrated some remarkable mechanical properties and long-term performance (e.g., high strength, chemical durability, and fire resistance). However, high drying shrinkage in AAC, causing cracks degrading the long-term durability of AAC, is one of the obstacles that must be overcome before it can be widely applied in the construction field.

This study investigates the mechanisms of drying shrinkage, provides a survey and evaluation of the influencing factors, and accordingly proposes an integral solution to mitigate drying shrinkage in AAC. This was done through a qualitative approach based on literary research.

The investigation showed that the main driving forces of drying shrinkage are surface, disjoining, and capillary tension forces, and they are related to relative humidity (RH) and meniscus radius. Further, different reaction products' characteristics can be attributed to different drying shrinkage mechanisms, as they have a critical role in determining AAC properties. Furthermore, poor mechanical properties of AAC often lead to a higher drying shrinkage rate. Surveying the influencing factors of drying shrinkage of AAC, in terms of raw materials, mix designs, and curing conditions showed their significant effect on drying shrinkage magnitude and mechanical properties. These factors were accordingly evaluated and systematized. Therefore, based on the survey and evaluation, a strategy was proposed to mitigate drying shrinkage in AAC.

Keywords: Alkali-activated concrete; AAC; Geopolymers; Drying shrinkage; Mechanism; Driving force; Pore size distribution; Relative humidity; C-A-S-H gel, N-A-S-H gel; Influencing factor; Activators; Admixture; Curing condition; Mitigation; Fly ash; Slag; Metakaolin

Contents

Preface	2
Abstract	3
1 Introduction	5
1.1 Alkali-activated concrete (AAC)	6
1.1.1 AAC main components	6
1.1.2 AAC classification	6
1.1.3 Pore structure	7
1.2 Drying shrinkage of AAC	8
2 The mechanisms of drying shrinkage of AAC	9
2.1 Driving forces	9
2.1.1 Surface energy	9
2.1.2 Disjoining pressure	9
2.1.3 Capillary pressure	9
2.2 Reaction products	10
2.3 Deformation resistance	11
3 The influencing factors of drying shrinkage of AAC	13
3.1 Precursors	13
3.2 Activators	14
3.3 Admixtures and Additives	15
3.4 Curing conditions	15
3.5 Overview of the influencing factors	16
4 Mitigation solutions	19
5 Conclusion	20
References	21
Appendix A	23
Appendix B	24

1 Introduction

The most consumed substance in the world after water is the conventional concrete (Aïtcin, 2000, as cited in Provis & Bernal, 2014). Ordinary Portland Cement (OPC) production is responsible for the emission of large quantities of carbon dioxide, as it contributes at least 5-8% of the total emissions worldwide (Scrivener and Kirkpatrick 2008, as cited in Li et al., 2019). It is therefore considered to be one of the major causes of global warming and atmospheric pollution (Hongqiang et al., 2019).

Alkali-Activated Concrete (AAC) appeared as an environmentally friendly alternative to conventional concrete (Z. Li et al., 2019). It is a cement-free concrete made from low-cost industrial by-products and alkali activators. Compared to cement, the gas emission of AAC is 0.18 t/t, while for cement is 1 t/t.; as for the energy consumption, it is 1230 MJ/t for AAC and 3500 MJ/t for cement (G. Ye, personal communication, November 18, 2019). Therefore, AAC can reduce carbon emissions by 25-50% (Duxson et al., 2007, as cited in Hongqiang et al., 2019). In addition to sustainability, AAC has demonstrated remarkable properties in terms of durability, such as high strength, chemical durability, and fire resistance (Arbi et al. 2016; Juenger et al. 2011; Provis and Deventer 2009, as cited in Z. Li et al., 2019). So, it shows remarkable mechanical properties and long-term performance.

However, before AAC can be widely applied in the construction field, there are still obstacles to overcome. One of these obstacles is the dry shrinkage that causes cracks, which leads to the weakening of the mechanical properties of the concrete and deterioration in its long-term performance (Thomas et al., 2017).

This research intends to focus on the state-of-the-art on drying shrinkage of AAC, which covers the drying mechanisms, influencing factors, and mitigation strategies. This research will provide guidelines for the development of crack-resistant AAC in structural/non-structural applications. Following research objectives are set as guidelines to fulfill this aim:

- To figure out mechanisms of drying shrinkage of AAC.
- To survey influencing factors of drying shrinkage of AAC in terms of raw materials, mix designs, and curing conditions. The influence of such factors on the workability and mechanical properties of AAC will also be considered.
- Based on the survey, propose an integral solution to mitigate drying shrinkage of AAC.

These objectives will be fulfilled based on literary research and through a qualitative approach, where the studied research will be compared and evaluated.

The structure of this report is as follows. In Chapter 2, AAC's drying shrinkage mechanisms are investigated in terms of driving forces, reaction products, and mechanical properties. This is followed by Chapter 3, which provides a survey and evaluation of the influencing factors. Accordingly, in Chapter 4, a strategy to mitigate the drying shrinkage is suggested. Chapter 5 contains a conclusion to what was discussed in the report. Finally, Appendix A contains the process of reaction product formation, and Appendix B contains a list of the used terms in this report.

¹ College lecture (Special Cements II, Geopolymer concrete) from course Concrete Science and Technology CIE5110 at the Delft University of Technology.

1.1 Alkali-activated concrete (AAC)

Alkali-activated concrete is an alternative to OPC concrete. Unlike OPC concrete that consists of cement and water, AAC is completely cement-free. AAC consists of precursor(s), alkali solution, and aggregates.

1.1.1 AAC main components

The two main components of AAC are precursor(s), alkali solution. **Precursors** are raw materials in solid form, and in AAC, industrial by-products and/ or cleaned wastes are used as precursors. The Precursors contained aluminum silicates (Provis & Bernal, 2014). They are activated by adding an alkali solution to them, and then they participate in the chemical reaction, producing other compounds (Provis et al., 2009). The by-products used as precursors are usually either slag, fly-ash, or metakaolin.

- o Fly ash: "the solid by-product of coal-fired electricity generation; consists mainly of glassy, spherical aluminosilicate particles." (Provis & Bernal, 2014, p. 301).
- Blast furnace slag (BFS): "calcium silicate-based product removed from the top of molten iron during its extraction from ore in a blast furnace; usually rapidly cooled to a glassy state and ground for use in construction materials." (Provis & Bernal, 2014, p. 301).
- Metakaolin: "the crystallographically disordered layered product of dehydroxylation of kaolinite (an aluminosilicate clay) at a temperature of~450-800°C, below the temperature at which the material recrystallizes to form mullite." (Provis & Bernal, 2014, p. 301).

Alkali solution is in liquid form and consists of water mixed with alkaline activators. The most used activators are NaOH (sodium hydroxide) and waterglass (Sodium silicate) (Mastali et al., 2018). Furthermore, activator choice depends on the type of precursor. The most used activators are:

- o Alkali hydroxides (NaOH, KOH)
- o Alkali Silicates (waterglass, Na₂O(n)SiO₂, K₂O₃Si)
- o Alkali metal carbonates (Na₂CO₃)
- o Alkali metal sulfates (Na₂SO₄)
- o Combination of alkali hydroxides + waterglass.

1.1.2 AAC classification

Besides the ingredients, the alkali-activated materials (AAMs) are classified based on their calcium content. Therefore, it is classified as either a high-calcium-based system, a low-calcium-based system, or a blended system.

- High-calcium-based system (Ca/ (Si + Al)>1):
 - o Precursors: BFS
 - The chemical reaction needs relatively moderate alkaline condition, room temperature
 - Reaction products: C-S-H type gel with a significant degree of aluminum substitution (C-A-S-H) as the main reaction product.
- Low-calcium (Aluminosilicate)-based system, so-called geopolymers:
 - o Precursors: metakaolin or fly ash (class F),
 - o The chemical reaction needs high alkaline condition and 60-80 °C
 - o Reaction products: Sodium aluminosilicate gel (N-A-S-H).
- **Blended system**, also called hybrid alkaline cement
 - o Precursors: mixing high-calcium-based and aluminosilicate-based precursor
 - The chemical reaction needs moderate alkaline condition, room temperature

- o Reaction products: C-A-S-H or a coexistence of C-A-S-H and N-A-S-H
- o Sometimes use Portland cement to activate the system, very similar like ternary blended system.

1.1.3 Pore structure

Pores in concrete are divided into three Sections: macro-, meso- and micropores. The spaces between the original cement grains are called capillary pores, which include both macro- and mesopores that are supposed to be filled with water, While the micropores are part of the calcium silicate hydrate gel component in alkali-activated slag concrete, for example, (Collins & Sanjayan, 2000).

According to the International Union of Pure and Applied Chemistry (IUPAC) system, pore sizes classification is shown in Table 1 (Collins & Sanjayan, 2000). The pore size distribution classification may differ somewhat from one research to another, or the term may differ, so attention must be paid to this aspect. According to Hojati et al. (2019), large capillaries and macropores are larger than 50 nm, while mesopores are between 2 nm and 50 nm, and micropores are smaller than 2 nm (see Section 3.1, for more info. about the pore size distribution of AAC).

Table 1 IUPAC pore size classification (Collins & Sanjayan, 2000)

Pore description	Radius (nm)
Micropores	<1.25
Mesopores	1.25–25
Macropores	25–5000
Entrained air voids, entrapped air voids, preexisting microcracks	5000–50 000

1.2 Drying shrinkage of AAC

There are different types of shrinkage; their terminology may differ in literature, and this is due to the similarity of their mechanisms and the influencing factors in some cases. Among the types of shrinkage are plastic, chemical, autogenous, drying, carbonation shrinkage. This research deals with drying shrinkage, as it has been defined by more than one source as an irreversible volume decrease that mainly occurs due to the loss of internal water from the pore network due to evaporation and due to moisture removal during drying (Hongqiang et al., 2019; Mastali et al., 2018). The drying shrinkage cracking affect the mechanical properties and the long-term performance of AAC; this may be a major problem that may appear after construction (Mastali et al., 2018). Therefore, it is essential to understand this phenomenon to reduce it.

The literature provides many experimental results for different AACs. These results may differ depending on the mix design (slag, fly ash, and metakaolin content, and activators modulus, type, and concentration), the use of different measuring tools and methods, etc. However, several matched results and conclusions have been mentioned in most of the papers.

Most of the alkali-activated slag (AAS) concrete samples showed a higher drying shrinkage rate than that of OPC, but OPC showed a higher weight loss than AAS (Collins & Sanjayan, 2000; Hojati et al., 2019; Thomas et al., 2017; Ye & Radlińska, 2016). Thomas et al. (2017) pointed out that the weight loss was about half or less than OPC, but in (Ye et al., 2017), some samples showed more weight loss than OPC. This may be attributed to using different activators in these samples and the coarser pore structure (Ye et al., 2017). Several points have been proposed to explain the low water/weight loss in AAS samples. Ye et al., (2017) referred to the difficulty of evaporating water from the AAS's small pores. There was no correlation between drying shrinkage and the quantity of weight loss in AAS, unlike OPC, which showed a correlation between the two (Collins & Sanjayan, 2000; Hojati et al., 2019; Thomas et al., 2017; Ye et al., 2017).

According to Thomas et al. (2017) concerning early age, the drying shrinkage rate in AAS was not as fast as in alkali-activated fly-ash (AAF). AAF samples showed higher drying shrinkage than OPC, in addition to a high-water loss similar to the amount of water loss in OPC in some cases (Thomas et al., 2017). In contrast to AAS, AAF drying shrinkage showed a direct correlation with water loss (Thomas et al., 2017; Y. Ma & Ye, 2015). Compared with early-age, AAC showed less shrinkage in later-age in general (Thomas et al., 2017). As for alkali-activated metakaolin (AAMk) concrete, it showed a large drying shrinkage attributed to the metakaolin particles' shape and the large surface area, which increases the water demand (Kuenzel et al., 2012, as cited in Mastali et al., 2018).

To fully understand the drying shrinkage, the driving forces of drying shrinkage, the reaction product characteristics, as well as the mechanical properties of AAC must be known, including their elastic modulus, Poisson's ratio, and compressive strength; this is what will be mentioned below.

2 The mechanisms of drying shrinkage of AAC

This chapter studies the mechanisms of drying shrinkage of AAC that discussed in the literature. The main driving forces are investigated along with the related parameters. The impact of reaction products on determining the drying shrinkage mechanisms is also mentioned, in addition to an extensive explanation of the correlation between mechanical properties, driving forces, and the magnitude of AAC's drying shrinkage.

2.1 Driving forces

According to the literature, three dominant forces contribute to the drying shrinkage: surface energy, disjoining pressure, and capillary pressure (Hojati et al., 2019; Provis, et al., 2019; Thomas et al., 2017).

2.1.1 Surface energy

Some references refer to it by other terms, such as "surface tension" or "Gibbs-Bangham effect", or "Gibbs-Bangham effect", or "Gibbs-Bangham effect", or "Gibbs-Bangham effect", or "Gibbs-Bangham equation and Gibb's free energy (Thomas et al., 2017). This force arises due to the diffusion of absorbed water within the pores, so it depends mainly on the specific surface area of the pores (Hojati et al., 2019; Thomas et al., 2017). It is also related to relative humidity (RH) and is remarkably effective when RH is low (\approx 11%RH) (Hojati et al., 2019; Provis, et al., 2019; Thomas et al., 2017).

2.1.2 Disjoining pressure

This force is prevalent in pores smaller than 2 nm, as it is generated by the cohesive interaction (Hojati et al., 2019; Thomas et al., 2017). This interaction occurs between the surface within the pore volume and the pore water (Thomas et al., 2017). A cohesive interaction may be due to several forces, but mainly due to van der Waals forces (Thomas et al., 2017). Disjoining pressure is also related to RH (Hojati et al., 2019; Thomas et al., 2017); see below.

2.1.3 Capillary pressure

Capillary pressure is the most common force among other driving forces and the one most mentioned in the literature. Capillary stresses arise because of the loss of water and the formation of a meniscus in the pores, so the magnitude of this stresses depend on the pores that have been emptied (Collins & Sanjayan, 2000; Hojati et al., 2019; J. Ma & Dehn, 2017; Ye & Radlińska, 2016). What generates higher capillary stress is the formation of the meniscus in finer pores. On the contrary, larger pores generate lower capillary stresses due to the lower ratio of pore volume to surface area (J. Ma & Dehn, 2017; Thomas et al., 2017).

The Kelvin-Laplace equation is usually used to demonstrate the correlation between the different terms that are related to capillary tension forces (Mastali et al., 2018; Ye et al., 2017; Y. Ma & Ye, 2015; Ye & Radlińska, 2016):

$$P_{c} = -\frac{2\gamma \cdot \cos \theta}{r_{c}} = \rho_{l} \frac{RT}{M} \ln RH$$
 (1)

Where:

- Pc is the capillary pressure [MPa],
- ρ_1 is density of liquid [kg/m3],
- M is molar mass of liquid [kg/mol],

- R is the universal gas constant R=8.314 [J/ (mol K)],
- T is temperature [K],
- γ is surface tension between pore water and vapor due to the molecular interaction [N/m],
- θ is the contact angle denoting the hydrophilicity of pore wall [$^{\circ}$],
- r_c is capillary radius at the position of the meniscus (Kelvin radius) $[m]^2$.

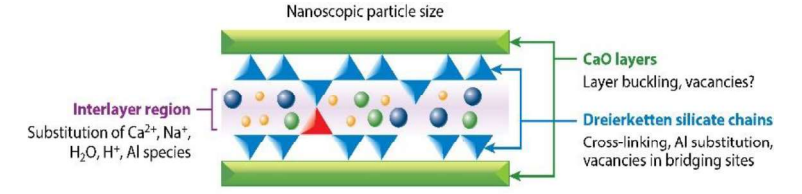
Ye et al. (2017) and Ye & Radlińska (2016) indicated that all pores with a radius smaller than Kelvin radius are filled with water at a certain RH, while larger pores are dry with layers of absorbed water adhering to the pore wall (Ye et al., 2017; Ye & Radlińska, 2016). Collins & Sanjayan (2000) referred to a hypothesis linking Kelvin radius to the shrinkage (but another term was used: r_s), namely that the lower r_c , the generate higher capillary tension forces at the meniscus, thus causing higher shrinkage. Collins & Sanjayan also concluded that if r_c is less than 16 nm, the shrinkage will increase rapidly in AAS. In (Ye et al., 2017; Ye & Radlińska, 2016), it has been indicated regardless of the pore size, the determination of r_c is mainly based on the RH and pore solution properties, and that in equilibrium conditions, the capillary pressure is mainly controlled by the RH

The different RH causes different shrinkage mechanisms (Ye & Radlińska, 2016), influencing the reaction products (Mastali et al., 2018). Eq.(1) indicates a correlation between capillary pressure, relative humidity, and meniscus radius (Ye et al., 2017; Ye & Radlińska, 2016). At high RH (≥ 50% RH), the capillary pressure was dominant, and conversely, at low RH, the dominant forces were surface energy and disjoining pressure (Hojati et al., 2019; Ye & Radlińska, 2016). So that with a decrease in the RH, the surface energy of the solid increases and the disjoining pressure increases in the solid phase between the absorbed water (Hu et al., 2019). According to Ye & Radlińska (2016), the highest AAS shrinkage was detected at 50% RH.

2.2 Reaction products

To explain the drying shrinkage mechanism sufficiently, knowledge of AAC's reaction product characteristics is therefore important. The main reaction product in AAC is either Calcium aluminosilicate hydrate (C-A-S-H) gel, Sodium aluminosilicate hydrate (N-A-S-H) gel, or both (Provis & Bernal, 2014).

The C-A-S-H gel is in the form of layers sheets with water in between (Mastali et al., 2018; Ye & Radlińska, 2016), Figure 1. Under drying, the structural incorporation of alkali cations in C-A-S-H makes it easier for C-A-S-H to collapse and redistribute and reduces the stacking regularity of its layers (Ye &



A Provis JL. Bernal SA. 2014. Figure 1 C-A-S-H gel structure (Provis & Bernal, 2014)

² It should be noted that Ye et al. (2017) used (r-t) in Eq.(1) instead of rc, where t refers to the thickness of adsorbed layer [m] and used $(\frac{\ln RH}{a_w})$ in Eq.(1) instead of $(\ln RH)$, where a_w refers to the water activity, accounting for the presence of ions in pore solution.

Radlińska, 2016). In this case, the rearrangement of the C-A-S-H nanoparticle structure is almost a permanent process, resulting in finer pores and irreversible deformation (Mastali et al., 2018; Ye & Radlińska, 2016). In this rearrangement, the driving forces have an essential role. At high RH (\geq 50%), The capillary pressure exerts forces on the C-A-S-H nanoparticles, compacting it, pulling the adjacent solids closer together, and reconstructing larger pores into smaller pores (Mastali et al., 2018; Ye & Radlińska, 2016). While at low RH (\approx 11%), other forces (such as surface energy) play a role in the shrinkage by stimulating the densification of the C-A-S-H particle itself (Mastali et al., 2018; Ye & Radlińska, 2016).

The C-A-S-H gel has a dense structure, fine pore structure, and good mechanical properties (Ye & Radlińska, 2016). In AAC (with C-A-S-H gel as the main reaction product), the high proportion of pores within the meso-and micropores and the few pores within the macropores lead to a direct drying effect and greater water loss within meso- and micropores. Which leads to the formation of meniscus within these fine pores (lower r_c) and generating higher capillary pressure (Collins & Sanjayan, 2000; J. Ma & Dehn, 2017; Thomas et al., 2017; Ye et al., 2017; Ye & Radlińska, 2016), as mentioned in Section 2.1.3.

The N-A-S-H gel has a three-dimensional structure (pseudozeolitic structure) and low reactivity (Garcia-Lodeiro et al., 2011; Šmilauer et al., 2011), Figure 2. It has a low ability to bind water chemically, and this causes an amount of water (that is not chemically bound to the aluminosilicate gel production) to be more prone to evaporate (Mastali et al., 2018; Šmilauer et al., 2011). Besides, the formation of the N-A-S-H gel as the main reaction product refers to higher total porosity and lower mechanical properties (Mastali et al., 2018; Ye & Radlińska, 2016). During the drying process, the water loss from these pores leads to the formation of the meniscus, which generates higher compressive stress in the capillary water on AAC's solid skeleton (Y. Ma & Ye, 2015).

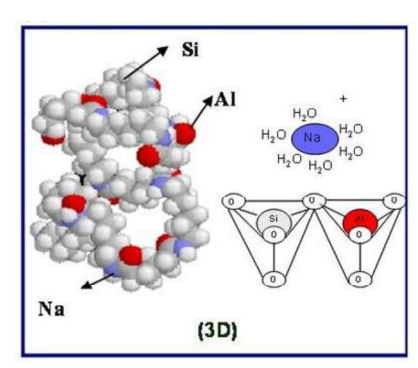


Figure 2 The three-dimensional structure of N-A-S-H gel (García-Lodeiro et al., 2012)

Accordingly, in both cases, regardless of the reaction products, as the driving forces (e.g. capillary pressure) increase, the drying shrinkage rate increases as well. However, the magnitude of the drying shrinkage also depends on the mechanical response to these forces. In the following Section, the correlation between the mechanical properties of AAC, driving forces, and drying shrinkage will be discussed.

2.3 Deformation resistance

The mechanical properties of AAC have a critical role in the shrinkage mechanisms since they represent the solid skeleton's resistance to deformation. In general, AAMs have a lower elastic modulus compared to OPC and a lower Poisson's ratio (Hojati et al., 2019; J. Ma & Dehn, 2017; Ye et al., 2017; Z. Li et al., 2020). Ye et al. (2017) pointed out that the elastic modulus may affect the shrinkage magnitude since it represents "the resistance of materials against elastic deformation when a force (e.g., capillary pressure) is applied" (Ye et al., 2017, p. 14).

The Mackenzie-Bentz's equation Eq.(2) and the bulk modulus equation Eq.(3) indicate the link between linear elastic shrinkage strain (ε_p), capillary pressure (σ_{cap}), and the bulk modulus of the paste (K) which in turn related the elastic modulus (E) and Poisson's ratio (v) (Hojati et al., 2019; Z. Li et al., 2020).

$$\varepsilon_p = \frac{D_s}{3} \sigma_{cap} \left[\frac{1}{K} - \frac{1}{K_s} \right] \tag{2}$$

Where:

- ε_p is linear elastic shrinkage strain,
- σ_{cap} is capillary pressure,
- Ds is the degree of saturation (or the saturation fraction),
- K the bulk modulus of the paste,
- K_s the bulk modulus of solid skeleton.

The degree of saturation Ds represents "the ratio between the evaporable water content and the total pore volume, and it determines how large fraction of solid was under the load of capillary pressure" (Bentz, Garboczi, and Quenard 1998, as cited in Z. Li et al., 2019, p. 154). According to Hojati et al. (2019), Ds is related to pore size distribution and pore solution properties, and "a higher D_s means more pores are capable of exerting shrinkage-inducing capillary forces to the solid skeleton, and accordingly, a larger drying" (Hojati et al., 2019). However, the increase in drying shrinkage does not depend only on one factor. As the degree of saturation increases, the capillary pressure may decrease, which could decrease the shrinkage. It should be noted that AAS is more sensitive to Ds change than AAF due to its finer pore structure (Thomas et al., 2017).

$$K = \frac{E}{3(1 - 2\nu)} \tag{3}$$

Where:

- K the bulk modulus of the paste,
- E the elastic modulus,
- υ Poisson's ratio.

Based on Eq.(2) and Eq.(3), it can be attributed that the lower the elastic modulus and the bulk modulus of the paste, the higher the drying shrinkage. Experimental results in the literature supported this. According to Ye et al. (2017), the samples with 33% lower bulk modulus showed 1.5 times larger drying shrinkage.

As mentioned before in Section 2.2 and will be mentioned extensively in Chapter 3, the mechanical properties in AACs could be different due to several factors, including the reaction products. This could explain the different and high magnitude of dry shrinkage in AAC. The presence of many influencing factors such as the content and nature of raw materials, alkali solution, liquid/ solid ratio, and curing conditions makes the chemical process in AAC very complex. The following chapter discusses the effect of these factors on drying shrinkage.

3 The influencing factors of drying shrinkage of AAC

This chapter will survey the influencing factors of drying shrinkage of AAC in terms of raw materials, activators, admixtures/ or additives, and curing conditions. Furthermore, the influence of such factors on AAC's workability and mechanical properties will also be considered. After surveying and evaluating these factors, they will be systematized into tables.

3.1 Precursors

AAMs' types and properties are an essential factor in the shrinkage mechanisms since they determine the main reaction product (C-A-S-H, N-A-S-H, or both), thus determining the mechanical properties (Ismail et al., 2014; Yip et al., 2005, as cited in Mastali et al., 2018; Ye et al., 2017; Ye & Radlińska, 2016). The high Ca-content in AAMs leads to C-A-S-H gel formation as the main reaction product, such as in slag (Ismail et al., 2014; Yip et al., 2005, as cited in Mastali et al., 2018). Conversely, the low Ca content leads to N-A-S-H gel formation as the main reaction product, and this is in some types of fly ash and metakaolin (Mastali et al., 2018). As the Ca content increases, the main reaction product can change from N-A-S-H to C-A-S-H gel, which means denser microstructure, better mechanical properties, and better results in terms of shrinkage behavior (Lecomte et al., 2006, as cited in Mastali et al., 2018). Conversely, low Ca content generally results in lower compressive strength and lower mechanical properties (Mastali et al., 2018). Appendix A shows an illustration of the hydration process and the formation of the reaction products (C-A-S-H- and N-A-S-H-gel).

The chemical properties are not the only important factor, but the physical properties also affect. For example, the slag particles' size leads to finer pores, while the spherical shape of fly ash with microaggregate increases the dimensional stability, and metakaolin particles increase the water demand (Mastali et al., 2018).

Collins & Sanjayan (2000) reported the importance of AAC's pore size distribution on drying shrinkage mechanisms. It has been found that AAS is more homogeneous in terms of the distribution of reaction products and that the distribution of the pores varies in a small range when compared with OPC (J. Ma & Dehn, 2017). Besides, when the slag content of concrete samples was increased, the pore size distribution became finer (Collins & Sanjayan, 2000). When comparing the OPC and the AAS, it was found that the proportion of pores within the micropores in the AAS tends to be higher than in the OPC, on the contrary, the pores within the capillary pores in AAS are less than in OPC (Collins & Sanjayan, 2000). It was also found that the values of r_c (Kalvin radius) of AAS are within the mesopores range, while OPC values of r_c are larger than the mesopores (Collins & Sanjayan, 2000). This means that meniscus form in smaller pores, thus generating higher capillary pressure, as mentioned in Section 2.1.3. According to Shi (as cited in Collins & Sanjayan, 2000), AAS has a pore size of less than 10 nm or more than 200 nm, while in OPC, it was found that the pore size distribution is more continuous, which is from 5 nm to 1200 nm (Collins & Sanjayan, 2000). The incremental pore size distribution data analysis shows that the percentage of pores within the mesopore classification ranges from 74.0% to 82.0% for AAS paste compared to 24.7 - 36.4% for OPC paste (Collins & Sanjayan, 2000). As for AAF, Thomas et al. (2017) indicated that very high porosity was observed in the AAF. These pores contained some large cavities but did not contain large capillary pores (Thomas et al., 2017). Hojati et al. (2019) indicated that AAC rich in fly ash has a higher porosity that may reach twice as high as AAC rich in slag, while OPC has an intermediate porosity. By comparison between different samples of AAF concrete, the sample that showed the least shrinkage had the coarsest pore structure and the least micropores, while the sample that showed the highest shrinkage had the largest volume of micropores and the highest specific pore surface area (Hojati et al., 2019). These

results may be related to using different types or concentrations of activators; this will be explained in Section 3.2.

As mentioned before, AAC properties may differ according to its reaction product, which depends on the chemical composition of the used precursor, especially fly ash and metakaolin. Slag-rich concrete has fine pore, dense matrix, high compressive strength, good mechanical properties, but has a high shrinkage rate, poor workability, insufficient setting time, and rapid slump loss (Humad et al., 2019; Mastali et al., 2018). These properties increase with increasing slag content and decrease by partial replacement of the slag with other precursors (Mastali et al., 2018). Fly ash-rich concrete has a high total porosity, low reactivity, low compressive strength, and poor mechanical properties (low modulus of elasticity and low passion ratio) (Mastali et al., 2018). Also, increasing the fly ash content in slag/ fly-ash blended systems leads to reducing compressive strength and mechanical properties (Škvára et al., 2003; Lee and Lee, 2013; Nath and Sarker, 2014; Criado et al., 2016; Liu et al., 2016, as cited in Humad et al., 2019). However, it improves workability, delays setting time, enhances the hardened matrix homogeneity, and limits microcracking (Wardhono et al., 2015; Humad et al., 2019). As for metakaolin, it is classified within the low Ca content, and its main reaction product is N-A-S-H gel (Mastali et al., 2018). It has high porosity and high-water demand, associated with relatively high dry shrinkage and crack formation (Mastali et al., 2018).

3.2 Activators

The most used alkali solution consists of a combination of sodium hydroxide (NaOH) and sodium silicate (Na₂SiO₃) known as waterglass (Mastali et al., 2018), but other types of activators are also used as mentioned in Section 1.1. Alkali activators raise the reaction mixture's pH value, facilitate the dissolution, and activates the hydration process (Mastali et al., 2018; Provis & Bernal, 2014). Therefore, activators type, modulus, and concentration can change the mixture's mechanical properties, pore structure, and microstructure (Mastali et al., 2018; Thomas et al., 2017). Thus, they have a major effect on mechanical properties and drying shrinkage (Ye et al., 2017), as well as an influence on the workability and setting time of the AAC (Mastali et al., 2018). The type of activators in the mixture depends mainly on the used precursors.

Increasing the amount of sodium silicate intensifies the hydration process, thus reducing the total porosity and the mesopores volume, leading to increased shrinkage in slag-rich concrete (Hu et al., 2019; Mastali et al., 2018; Thomas et al., 2017). Besides, AAS concrete activated by sodium silicate showed lower workability and slump loss (F. G. Collins & Sanjayan, 1999). In comparison between the use of NaOH and waterglass to activate the samples or the use of NaOH alone, the use of NaOH and waterglass together showed a finer pore structure in AAS (Ye et al., 2017). Ye et al. (2017) indicated an increase in the silicate dosage associated with the finer pore structure. Increasing the silica modulus (SiO₂/Na₂O) increases the compressive strength but causes finer pores to form, which increases the capillary tension, leading to an increase in the drying shrinkage rate in AAS (Mastali et al., 2018; Thomas et al., 2017). The increase of NaOH concentration leads to a stronger and denser structure, which increases the compressive strength and reduces the drying shrinkage rate in AAF (Atiş et al., 2015, as cited in Mastali et al., 2018). However, its increase in AAS will increase the drying shrinkage (Ye et al., 2017).

The increase or decrease of the activators' content, modulus ratio, or liquid/binder ratio must be within a certain limit; otherwise, this increase or decrease can give the opposite results. In this report, no specific values are mentioned because of the need to review more data and because there is no experimental aspect of this research.

3.3 Admixtures and Additives

Additives or admixtures are used to obtain some of the mixture's desired properties, and the literature states that they can also give good results in terms of shrinkage behavior, mechanical properties, and workability (Mastali et al., 2018). The type of additive/ admixture may be different depending on the mixture's components, and the shrinkage may be increased or decreased depending on the use of different additives or admixtures. Here are some of the admixtures/additives used in AAC:

- The use of **nano-TiO**₂ in AAC accelerates the hydration process, resulting in producing more reaction products and denser structure. Thus, it may increase compressive strength and decrease dry shrinkage in both AAS and AAF (Duan et al., 2016, as cited in Mastali et al., 2018).
- Using **magnesia** (**MgO**) also accelerates the hydration process and fills the pores (Mastali et al., 2018). It reduced shrinkage in AAS and improved the crack resistance of slag/ fly-ash concrete (Fang et al., 2010, as cited in Mastali et al., 2018). But it was noted that the effect of MgO depends on its reactivity (Fang et al., 2010, as cited in Mastali et al., 2018).
- Expanding admixtures (EA) reduce dry shrinkage in AAS and increase compressive strength at early-age and reduce the setting time (Yang et al., 2017, as cited in Mastali et al., 2018). EA's main minerals are quick lime, anhydrite, periclase, and portlandite (Yang et al., 2017, as cited in Mastali et al., 2018).
- It was also found that the addition of **gypsum, common air-entraining admixtures (AEA)**, and **shrinkage-reducing agent (SRA)** in AAS reduces the magnitude of the dry shrinkage (Thomas et al., 2017). The addition of SRA significantly reduced the drying shrinkage due to decreased capillary pressure and mass loss after its addition (Hu et al., 2019). The use of higher dosages of SRA showed a clear difference in the results of the drying shrinkage (1100 μm/m with 3% SRA to 1300 μm/m with 1% SRA) (Jia et al., 2018, as cited in Mastali et al., 2018).
- For AAMk, the addition of either calcite (CaCO₃) or dolomite CaMg(CO₃)₂ improved the mechanical properties but increased the shrinkage (Yip et al., 2008, as cited in Mastali et al., 2018). The addition of ammonium molybdate resulted in a decrease in the shrinkage rate but exceeding it more than 1.57% led to undesirable results in terms of the materials' hardening mechanism (Vidal et al., 2015, as cited in Mastali et al., 2018).

3.4 Curing conditions

Curing conditions and the RH significantly affect the rate of drying shrinkage in AAC (Mastali et al., 2018; Thomas et al., 2017). The drying shrinkage of AAC is significantly reduced when steam- or heat-cured (Hojati et al., 2019; Thomas et al., 2017). When AAC was moist cured at 26 ° C, the shrinkage rate was still high. But the 28-d strength was improved, especially for fly ash-rich mixtures (Hojati et al., 2019). However, when AAC was steam cured at 60 ° C, the shrinkage was reduced in the fly ash-rich mixtures, unlike the slag-rich mixtures, which was slightly affected (Hojati et al., 2019). It should be noted that steam curing greatly improved the 28-d strength of the fly ash-rich mixture; besides, it showed improvement in its bulk elastic modulus (Hojati et al., 2019).

Thomas et al. (2017) indicated that heat curing or moist curing³ reduced drying shrinkage in AAC containing slag or fly ash, improved the volumetric stability of AAC, increased compressive strength, and dynamic modulus of elasticity, especially for fly ash. Further, Bakharev et al. (as cited in Mastali et al., 2018) indicated that heat curing reduced dry shrinkage in AAS and increased the compressive strength at

³ moist curing for 72h then submerging in saturated limewater for 90d instead of 48 h before to drying

early-age but decreased at later-age (compared to curing at ambient temperature) (Mastali et al., 2018). Marjanovic' et al. (as cited in Mastali et al., 2018) found that curing AAC samples ($\frac{1}{4}$ fly ash, $\frac{3}{4}$ slag) at 95 °C for 24 hours significantly reduced the drying shrinkage compared to curing at 20 °C for 24-hour (1000 μ m/m at 95° C, 4500 μ m /m at 20° C, 800 μ m/m OPC at 20° C). Besides this, Thomas et al. (2017) indicated that heat-curing for shorter durations of AAC is expected to show significant strength development.

Curing time and temperature reduces the total porosity, pore size, and pore connectivity of AAC (Thomas et al., 2017). Also, AAC curing at elevated temperature affect the reaction product and accelerate hydration (Mastali et al., 2018; Thomas et al., 2017). Therefore, curing time and temperature under specific curing conditions affects the hydration process and changes the pores structure, the microstructure, and mechanical properties. Thus, the drying shrinkage, the compressive strength, and cracking will increase or decrease (Mastali et al., 2018; Thomas et al., 2017). In general, moist curing is essential for AAC regardless of the mixture content. However, heat curing is necessary for fly ash-rich concrete (as the main reaction product is N-A-S-H gel) since it increases its reactivity.

3.5 Overview of the influencing factors

In the next tables, the influencing factors were collected in a systematic manner. They show the influence of precursors, activators, admixtures, and additives, and curing conditions on AAC mixture. S, FA, and Mk refer to slag, fly-ash, and metakaolin, respectively. High, medium, and low in Table 2 means, for example, that AAS has high compressive strength compared to AAF, which has low compressive strength. ↑ and ↓ means that the partial replacement of slag with fly-ash will reduce drying shrinkage. While in Table 3 and Table 4 means that the use of x-activator or y-admixture will increase or decrease drying shrinkage. In Table 5, high, low, and medium means, for example, that heat-curing has a higher effect on fly ash-rich concrete compared to moist-curing.

 $Table\ 2\ The\ influence\ of\ precursors\ with\ partial\ replacement\ on\ AAC\ properties\ and\ drying\ shrinkage.$

Pre	ecursor	Read prod			Dense structure	Pores structure		Compressive	Mechanical	Drying		Setting	
Main	Partial replacement with	Main	Other	Reactivity		Porosity	fineness	strength	properties	shrinkage	Workability	time	additional
S		CASH			High		High	High	medium	High	Low	Low	
FA		NASH	CASH	Low		High		Low	Low	High	High	High	depends on Ca content
Mk		NASH		Low		High		Low	Low	High			
S	FA	CASH	NASH			1	↓	V		\	↑	↑	
3	Mk	CASH	NASH							+			
FA	S	NASH	CASH	↑	1		1	^	↑	1			
Mk	FA	NASH	CASH					↑		\			FA with high Ca content

Table 3 The influence of some activators on drying shrinkage and properties of AAC containing different precursors type.

Activators	Precursor	Hydration process	Dense structure	Pores st	fineness	Compressive strength	Mechanical properties	Drying shrinkage	Workability	Setting time	additional
NaOH	S FA	p. cccss	<u>↑</u>	↓	↑	1	↑	↑			
waterglass	S For all	Λ		↑				↑	4		slump loss
waterglass and NaOH	-	'		1	↑			↑			compared to using NaOH alone
Silica modulus	S				↑	↑		↑			

 $Table\ 4\ The\ influence\ of\ some\ admixtures/\ additives\ on\ drying\ shrinkage\ and\ properties\ of\ AAC\ containing\ different\ precursor\ type.$

Admixtures/ Additives	Precursor	Hydration process	Dense structure	Pores st Porosity	fineness	Compressive strength	Mechanical properties	Drying shrinkage	Workability	Setting time	additional			
nano-TiO2	S	_	_	1	_				1		→			
110110-1102	FA	l	l			1		\downarrow						
MgO	S	↑						→			improved the crack resistance of slag/ fly-ash concrete			
AEA	S							\downarrow						
SRA	S							V						
EA	S	\uparrow				^	↑	→		→				
EA	FA							\rightarrow						
Steel fibers	For all						↑	\rightarrow						
Sand	For all							\			sand to binder ratio from 0 to 1			
calcite or dolomite	Mk						↑	^						
ammonium molybdate	Mk							\						

Table 5 The effect of curing on AAC compared to different conditions.

Curing conditions	AAMs	Compressive strength	Mechanical properties	Drying shrinkage				
	S	Low		Low				
Moist-curing	FA	Medium		Low				
	For all	Medium						
Steam-curing	S	Medium		Medium				
Steam-curing	FA	High	Medium	Medium				
Heat curing	S	medium		Medium				
Heat-curing	FA	High	High	High				

4 Mitigation solutions

Mitigation strategies of drying shrinkage can be proposed after understanding of drying shrinkage mechanisms of AAC and knowing the influencing factors. As mentioned before, the drying shrinkage is a complex process, and it is related to AAC properties. Note that the selection of AAC components is related to the specifications desired to be achieved with the concrete (e.g., high strength, chemical durability, and fire resistance). Based on the survey of the influencing factors in Chapter 3, some strategies can be suggested to mitigate AAC's drying shrinkage. Most of the survey results were collected in Section 3.5. Here are some suggestions based on these results:

- Using a combination of different precursors gives better results in terms of drying shrinkage, compressive strength, and workability, see Table 2. For example, partial replacement of slag with fly ash improves workability and reduces drying shrinkage by increasing its porosity (Mastali et al., 2018). But it causes reducing the compressive strength. Therefore, this solution may not be ideal if high compressive strength is required. In general, using the blended system gives better results in terms of dry shrinkage and crack resistance.
- The choice of activator depends on the type of precursor used for the reaction. The use of the appropriate concentration, modulus, and ratio of the activators increases the reaction's efficiency. This is especially important for fly ash and metakaolin due to their low reactivity and calcium content. Therefore, there is a need for what accelerates the hydration process, increases the calcium content, reduces porosity, and increases the structure's density. The use of NaOH gave positive results to fly ash as a precursor (see Table 3, for more).
- As for admixtures/ additives, their use in the mixture gave positive results, especially for slag-rich concrete. Several admixtures were used in AAC that reduced the rate of shrinkage, increased compressive strength or improved workability (see Section 3.2 and Table 4, for more).
- One of the additives that gave successful results is the addition of fiber, especially steel fibers. Adding steel fibers improved mechanical properties and reduced drying shrinkage in AAC (Ranjbar et al., 2016, as cited in Mastali et al., 2018). Also, increasing sand/ binder ratio from 0 to 1 reduced the drying shrinkage in AAC containing FA and Mk (Mastali et al., 2018).
- Moist-curing is important for AAC, as it controls the drying shrinkage, although it has not reduced it significantly (see table 4). But for fly ash-rich concrete, curing at ambient temperature is usually needed since heat-curing accelerates the chemical reaction.

Besides the correlation between the formation of reaction products and the Ca content (see Section 3.1, for more), the Ca content is also related to the strength development, elastic modulus E, setting time, and shrinkage behavior (Mastali et al., 2018). The high shrinkage rate in AAC may also be attributed to a low Ca/Si ratio (J. Ma & Dehn, 2017; Mastali et al., 2018). Mastali et al. (2018) mentioned the impact of the molar ratio of (Ca/Si, Al/Si, Na/Si, and Mg/Si) on the shrinkage behavior and sorted it according to the following order, from highest to lowest: Ca/Si > Al/Si > Mg/Si > Na/Si. Therefore, one of the solutions that may be suggested is to increase the Ca content in low-Ca mixtures (e.g., fly-ash and metakaolin), which enhances the mechanical properties and the microstructure. Further, the silicates reduction may also reduce the drying shrinkage in AAC (Mastali et al., 2018). The decrease or increase of the silicate or calcium content can be done by using certain types of activators, or additives and admixtures.

5 Conclusion

In this paper, the mechanisms of drying shrinkage in AAC were investigated. Further, the influencing factors of drying shrinkage were surveyed and evaluated and accordingly systematized, see Section 3.5. Based on that, mitigation strategies of drying shrinkage were proposed.

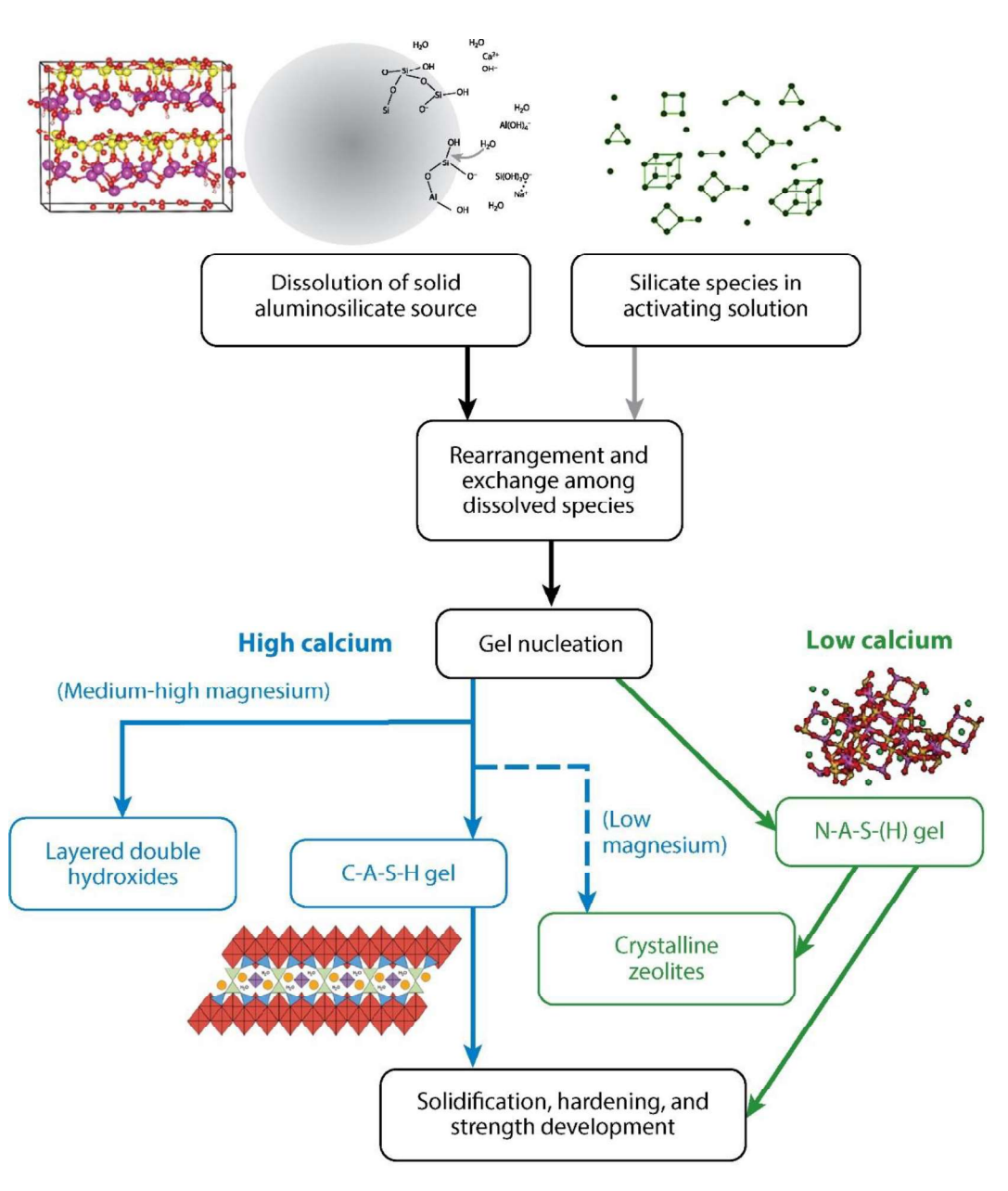
- 1. In general, AAC exhibited a higher drying shrinkage rate than conventional concrete.
- 2. Investigation of drying shrinkage mechanisms of AAC shows the main driving forces of drying shrinkage are surface, disjoining, and capillary forces.
- 3. Drying at different RH causes different drying shrinkage mechanisms as well. At high RH (≥ 50% RH), the capillary tension force is dominant, while at lower RH, disjoining- and surface tension forces are dominant.
- 4. During the drying process, menisci will be formed (interface between water and air), which generates tensile forces in the capillary water, pulling the nanoparticles of the material closer to each other, causing deformation. The tensile forces (capillary pressure) increase with the increase in the total porosity or fineness of the AAC pore structure. Therefore, the mesopores volume and the meniscus radius are important in determining the shrinkage magnitude.
- 5. The reaction product characteristics have a critical role in determining the AAC properties. Moreover, the magnitude of drying shrinkage depends on the AAC resistance to deformation due to the driving forces, and the mechanical properties of AAC represent this resistance (e.g., compressive strength, elastic modulus E, bulk modulus K, Poisson's ratio v, etc.). Poor mechanical properties (such as low elastic modulus) often lead to a higher drying shrinkage rate.
- 6. The influencing factors (e.g., precursors, activators, admixtures/ or additives, curing conditions) have a great impact on the hydration process and the reaction products, which affect the microstructure, pore structure, and mechanical properties of AAC, and thus affect the magnitude of the drying shrinkage, Table 2, Table 3, Table 4, and Table 5.
- 7. Mitigation solutions are based on the understanding of drying shrinkage mechanisms and the influencing factors, Chapter 4. The mitigation strategy depends mainly on using a combination of precursors with the compatible type and concentration of activators. Besides, using admixtures or additives to achieve better results in terms of drying shrinkage, mechanical properties, and workability. Moreover, curing must be applied to control drying shrinkage, considering the convenient curing conditions for each AAC type, such as heat-curing for fly ash-rich concrete.

References

- Aïtcin, P. C. (2000). Cements of yesterday and today concrete of tomorrow. *Cement and Concrete Research*, 30(9), 1349–1359. https://doi.org/10.1016/S0008-8846(00)00365-3
- Collins, F. G., & Sanjayan, J. G. (1999). Workability and mechanical properties of alkali activated slag concrete. *Cement and concrete research*, 29(3), 455-458.
- Collins, F., & Sanjayan, J. G. (2000). Effect of pore size distribution on drying shrinkage of alkaliactivated slag concrete. *Cement and Concrete Research*, 30(9), 1401–1406. https://doi.org/10.1016/S0008-8846(00)00327-6
- Garcia-Lodeiro, I., Palomo, A., Fernández-Jiménez, A., & MacPhee, D. E. (2011). Compatibility studies between N-A-S-H and C-A-S-H gels. Study in the ternary diagram Na2O-CaO-Al2O3-SiO 2-H2O. *Cement and Concrete Research*, 41(9), 923–931. https://doi.org/10.1016/j.cemconres.2011.05.006
- Hojati, M., Rajabipour, F., & Radlińska, A. (2019). Drying shrinkage of alkali-activated cements: effect of humidity and curing temperature. *Materials and Structures/Materiaux et Constructions*, 52(6). https://doi.org/10.1617/s11527-019-1430-1
- Hongqiang, M., Hongyu, C., Hongguang, Z., yangyang, S., Yadong, N., Qingjie, H., & Zetao, H. (2019). Study on the drying shrinkage of alkali-activated coal gangue-slag mortar and its mechanisms. *Construction and Building Materials*, 225, 204–213. https://doi.org/10.1016/j.conbuildmat.2019.07.258
- Hu, X., Shi, C., Zhang, Z., & Hu, Z. (2019). Autogenous and drying shrinkage of alkali-activated slag mortars. *Journal of the American Ceramic Society*, 102(8), 4963–4975. https://doi.org/10.1111/jace.16349
- Humad, A. M., Kothari, A., Provis, J. L., & Cwirzen, A. (2019). The effect of blast furnace slag/fly ash ratio on setting, strength, and shrinkage of alkali-activated pastes and concretes. *Frontiers in Materials*, 6(February), 1–10. https://doi.org/10.3389/fmats.2019.00009
- Humad, A. M., Provis, J. L., & Cwirzen, A. (2019). Effects of Curing Conditions on Shrinkage of Alkali-Activated High-MgO Swedish Slag Concrete. *Frontiers in Materials*, 6. https://doi.org/10.3389/fmats.2019.00287
- Li, J., Yu, Q., Huang, H., & Yin, S. (2019). Difference in the reaction process of slag activated by waterglass solution and NaOH solution. *Structural Concrete*, 20(5), 1528–1540. https://doi.org/10.1002/suco.201900130
- Li, Z., Liu, J., & Ye, G. (2019). Drying shrinkage of alkali-activated slag and fly ash concrete; A comparative study with ordinary Portland cement concrete. *Heron*, 64(1–2), 149–163.
- Li, Z., Lu, T., Liang, X., Dong, H., & Ye, G. (2020). Mechanisms of autogenous shrinkage of alkaliactivated slag and fly ash pastes. *Cement and Concrete Research*, 135(May), 106107. https://doi.org/10.1016/j.cemconres.2020.106107
- Ma, J., & Dehn, F. (2017). Shrinkage and creep behavior of an alkali-activated slag concrete. *Structural Concrete*, 18(5), 801–810. https://doi.org/10.1002/suco.201600147
- Ma, Y., & Ye, G. (2015). The shrinkage of alkali activated fly ash. *Cement and Concrete Research*, 68, 75–82. https://doi.org/10.1016/j.cemconres.2014.10.024
- Mastali, M., Kinnunen, P., Dalvand, A., Mohammadi Firouz, R., & Illikainen, M. (2018). Drying shrinkage in alkali-activated binders A critical review. *Construction and Building Materials*, *190*, 533–550. https://doi.org/10.1016/j.conbuildmat.2018.09.125
- Provis, J. L., & Bernal, S. A. (2014). Geopolymers and related alkali-activated materials. Annual Review

- of Materials Research, 44, 299-327. https://doi.org/10.1146/annurev-matsci-070813-113515
- Provis, J. L., Deventer, J. S. J., & van Deventer, J. S. J. (2009). Geopolymers. Elsevier Gezondheidszorg. https://www.sciencedirect.com/book/9781845694494/geopolymers#book-description
- Šmilauer, V., Hlaváček, P., Škvára, F., Šulc, R., Kopecký, L., & Němeček, J. (2011). Micromechanical multiscale model for alkali activation of fly ash and metakaolin. *Journal of Materials Science*, 46(20), 6545–6555. https://doi.org/10.1007/s10853-011-5601-x
- Thomas, R. J., Lezama, D., & Peethamparan, S. (2017). On drying shrinkage in alkali-activated concrete: Improving dimensional stability by aging or heat-curing. *Cement and Concrete Research*, 91, 13—23. https://doi.org/10.1016/j.cemconres.2016.10.003
- Ye, H., Cartwright, C., Rajabipour, F., & Radlińska, A. (2017). Understanding the drying shrinkage performance of alkali-activated slag mortars. *Cement and Concrete Composites*, 76, 13–24. https://doi.org/10.1016/j.cemconcomp.2016.11.010
- Ye, H., & Radlińska, A. (2016). Shrinkage mechanisms of alkali-activated slag. *Cement and Concrete Research*, 88, 126–135. https://doi.org/10.1016/j.cemconres.2016.07.001

Appendix A



Provis JL, Bernal SA. 2014.
Annu. Rev. Mater. Res. 44:299–327

Figure 3 The formation process of the reaction products (C-A-S-H- and N-A-S-H-gel) (Provis & Bernal, 2014)

Appendix B

Table 6 list of the used terms

OPC	Ordinary Portland Cement
AAC	Alkali-Activated Concrete
AAMs	Alkali-activated materials
AAS	Alkali-activated slag
AAF	Alkali-activated fly-ash
AAMk	Alkali-activated metakaolin
RH	Relative humidity
C-A-S-H	Calcium silicate hydrate
N-A-S-H	Sodium aluminosilicate hydrate
EA	Expanding admixtures
AEA	Common air-entraining admixtures
SRA	Shrinkage-reducing agent